

D. DRENIĆ*, S. SEDMAK**, A. RADOVIĆ**

Side-grooved fatigue precracked DCB specimens of two different lengths, made of NIONICRAL 70, 800 MPa strength class steel, were tested on drop-weight testing machine in order to determine the crack velocity. For that purpose developed device consisted of timer with basic digital unit time of 86.4 ns and uniformly spaced connecting liquid silver strips obtained on paper-base insulating foil by screen process printing. Crack velocities ranged from about 439 m/s to 508 m/s at room temperatures and from 664 m/s to 717 m/s at -50°C . An effect of initial ligament length ratio was also observed in the fast fracture tests.

INTRODUCTION

Crack tip velocity is an important parameter in the fast fracture processes. The fast fracture toughness variation with respect to the crack velocity could be significant in these processes, Harn et al (1). The crack velocity generally depends on the material properties, the specimens shape and size and the testing conditions (e.g. loading speed, test temperature), Irwin (2). A simple method of a crack velocity measurement is in the crack tip position determination on the specimen surface at different times of fracture, Erdogan (3). Experimental determination of the crack velocity could be of a significant help in the dynamic fracture toughness tests.

This paper presents some results obtained with the DCB (Double Cantilever Beam) type specimens made of 800 MPa strength class steel in the impact tests on the drop-weight machine. The crack velocity was determined as a ratio of the uniformly spaced strip marked distances and the corresponding time periods, recorded during the fracture process on the, for that purpose developed, timer with memories.

INSTRUMENTATION

For impact loading of specimens a vertical drop-weight machine of 90 kg mass tup and 3.5 m maximum working height was used. Wedge loading arrangement is shown in Fig. 1. DCB type specimen

*Faculty of Civil Engineering, Niš, Yugoslavia

**Faculty of Technology and Metallurgy, Beograd, Yugoslavia

(1) is positioned on the machine anvil (2), over the rubber buffer (3). The specimen is held in the up-right position by two side-supports (4). Wedge-striker (5) with the 25° wedge angle has on its upper surface a reduced area in comparison with the tup (6) impact area. The wedge striker is introduced between symmetrically disposed hole-pins (7), which serve for impact load transfer. In order to minimize the friction, striker and pins are quenched and grinded.

Three main problems had to be solved in order to develop the crack velocity recording device. The first one was the time periods measuring, the second one was the crack tip position determination, and the third problem was how to connect the time and the distance recordings. A schematic view of the developed device is presented in Fig. 2a. The electronic device consists of a timer (1) with a time-base selector, a digital counter (2), a binary counter (3), memories (4) and two outputs for an oscilloscope (5) and a recorder (6). The minimal time-base of 86,4 ns is given by the built-in integrated circuits. There are 15 memories all together, and the last one (15th) marked the total integrated time for all separate time periods. The crack tip position is indicated by making use of 16 equidistant strip-marks (Fig. 2b), screen process printed by liquid silver plating on the paper-base insulating foil (7). This technique enables the minimum strip distance of 2.0 mm. Printed silver strips serve solely as connectors. Insulating foil was bonded on the specimen surface by using cement for strain gauges.

SPECIMENS

All tests in this experiment were performed on DCB specimens, made of NIONICRAL 70 steel, produced by Steel-works "Jesenice", Yugoslavia. The chemical analysis and mechanical properties of NIONICRAL 70 steel are listed in Table 1.

The preliminary experiments were performed on notched, fatigue precracked DCB specimens with smooth outer surface (Fig. 3a). The stress concentration, induced only by the fatigue crack, did not produce the state of plane strain, and after a short propagation along the initial direction, the crack deviated by 45°, exhibiting the plane stress condition (Fig. 3b). The crack arrest properties were clearly demonstrated in this experiment and cracks, obtained by impact, were short. These short and deviated cracks did not permit the correct positioning of silver-strip foil; thus the measuring of the crack velocity was impossible. The specimens were provided by the side grooves in order to achieve the plane strain condition (Fig. 4). This is an effective method to direct the crack propagation in the desired direction, through the reduced cross-section area, Hoagland (4).

Experiments were carried out with the side grooved specimens of two different lengths. The nominal length $W_A = 282,5$ mm of the "A" specimen was approximately calculated and treated as a standardized value. The first experiments with these standardized specimens have shown the high level of stored potential energy compared to kinetic energy of falling weight. The first impact was followed by back jump of the tup, which fell again

Table 1

Chemical Analysis and Mechanical Properties of NIONICRAL 70 Steel

A. Chemical Analysis											(wt, %)
C	Si	Mn	P	S	Cr	Ni	Mo	V	Al	N	
0.11	0.14	0.25	0.010	0.016	1.26	2.84	0.29	0.070	0.060	0.011	

B. Tensile Properties

Yield stress	Ultimate tensile stress	Elongation	Contraction
Y.S.	U.T.S.	δ	ψ
MPa	Mpa	%	%
300	844	16.6	64.2

C. Charpy V Impact Energy

Test temperature	°C						
	20	-20	-40	-60	-30		
Absorbed energy	J	L*	129	128	125	119	116
		T*	87	84	87	84	77

*L denotes rolling direction and T denotes transverse direction

D. ASTM E208 NDT Temperature

Specimen	P3	
NDT Temperature	°C	-103

breaking the specimen. This was demonstrated in a plot of strain variations in time, recorded by strain gauge M1 (Fig. 5). In order to reduce the specimen resistance, the nominal length of the specimen was reduced to about $W_B = 185.5$ mm (2/3 of W_A) and these specimens are treated as short and marked "B". It could be concluded from the short specimen plot (Fig. 6) that jump effect was missed. The specimens were not completely broken in this experiment. It is interesting to note the strains on the strain gauge M3 position remote from the initial crack tip. The standard and short specimen plots are similar. When the crack tip overpasses certain position determined by fracture process variables, the strain remains unchanged.

EXPERIMENTS AND RESULTS

The crack velocities were determined for both "A" and "B" specimens, which have different initial ligament lengths, at two different test temperatures (room temperature and -50°C) and for different impact energies (corresponding to six different tup heights, ranged from 1 m to 3.5 m). The cracks propagated partly in all experiments and the tests were performed under crack arrest condition.

Different impact energies and different tup speeds were introduced in the first series of experiments by changing the

Table 2. Crack lengths and recorded times for different impact energies

Initial tup height level	Impact energy	Crack lengths				Recorded time				
		Final/For recorded time				Specimen Nr				
						Average value		Specimen Nr		Average value
		1	2	3		1	2	3		
m	J	mm				s				
Specimen "A" - 245 mm ligament length										
1	883	8/8	10/10	9/8	9/8.7	25	28	25	26	
1.5	1324	21/20	22/22	17/16	20/19.3	46	49	46	47	
2	1766	39/36	40/40	32/32	37/36	77	79	72	76	
2.5	2207	50/48	54/52	52/52	52/50.7	108	116	112	112	
3	2649	72/72	62/60	76/72	70/68	151	147	152	150	
3.5	3090	78/78	85/84	78/78	80/78	191	188	164	181	
Specimen "B" - 148 mm ligament length										
1	883	11/10	12/12	13/12	12/11.3	30	28	26	28	
1.5	1324	26/26	24/24	22/22	24/24	53	50	47	50	
2	1766	40/40	37/36	40/40	39/38.7	80	71	81	77.3	
2.5	2207	54/52	58/56	56/56	56/54.7	122	130	126	126	
3	2649	72/72	72/72	72/72	72/72	152	152	152	152	
3.5	3090	119/110	112/110	119/110	116.7/110	235	237	236	236	

initial tup height. The tests were performed at room temperature, with side-grooved "A" and "B" specimens. The crack lengths, obtained in these experiments for different impact energies, and also the time periods corresponding to the last broken strip on the bonded foil, are shown in Table 2.

The second part of the experiment consisted of tests, performed on "A" and "B" specimens at the full machine capacity (tup mass of $m=90$ kg, height level of $h=3.5$ m, impact velocity of $v=8.28$ m/s and tup energy of $E=3090$ J). Temperature effect was investigated by testing at two different temperatures (room temperature and -50°C). Crack length of maximum 150 mm could be measured by the strip foils, consisted of 16 silver strips disposed each 10 mm. Zero strip was positioned at the initial crack tip. The measuring range of 150 mm was sufficient to cover all crack extensions, obtained in four experiments, as it can be seen in Tables 3 and 4. The available tip energy was sufficient only for partial separation of broken specimen parts. The final crack lengths, obtained in these experiments, are indicated in Tables 3 and 4 also. The basic recorded time was, as mentioned already, 86.4 ns.

DISCUSSION

The analysis of experimental data, presented in Tables 2, 3 and 4, is summarized in Fig. 7, 8 and 9.

Table 3. Crack extensions and recorded times for 90 kg tup impact energy of 3090 J at room temperature

Memory number	Strip distance (from zero)	Recorded time for specimen			Average value
		1	2	3	
	mm	μs			μs
Specimen "A" - 245 mm ligament length					
1	10	19	23	21	21
2	20	38	39	40	39
3	30	63	65	61	63
4	40	88	80	81	84
5	50	108	104	106	106
6	60	125	120	121	122
7	70	140	148	147	145
8	80	169	178	176	174
Final crack length, mm		82	81	87	83
Specimen "B" - 148 mm ligament length					
1	10	18	22	17	19
2	20	37	44	39	40
3	30	60	57	54	57
4	40	80	75	79	78
5	50	101	95	95	97
6	60	118	122	111	117
7	70	134	139	141	138
8	80	162	168	168	166
9	90	203	209	203	205
10	100	224	223	224	224
11	110	235	237	236	236
Final crack length, mm		119	112	119	117

The crack extension vs impact energy dependences for "A" and "B" specimens are drawn in Fig. 7. For the same impact energy, the larger crack extension was obtained with shorter initial specimen ligaments. This could be contributed to the higher loading capacity of longer specimen ligament, but the effect of ligament length on stress state, specimen compliance and crack resistance has to be taken into account as well, Knott (5).

The impact energy vs. crack extension dependence is not a linear one, and this could be explained by combined effect of the stress concentration (caused by fatigue crack and side grooves) and impact speed, on the fast fracture. Recorded times for measured crack extension in Table 2 enabled the crack velocity determination, presented by diagrams in Fig. 8. The crack extension in time is expressed by regression line of general form

$$y = mx + b, \quad (1)$$

where y stands for variable crack extension $a-a_0$, and where a , a_0 denote the instantaneous and initial crack lengths, respectively. x stands for measured time t and m and b are coefficients. Calculating coefficients m and b two regression line

Table 4. Crack extensions and recorded times for 90 kg tup impact energy of 3090 J at -50°C

Memory number	Strip distance (from zero)	Recorded time for specimen			Average value
		1	2	3	
mm		μs			μs
Specimen "A" - 245 mm ligament length					
1	10	15	12	12	13
2	20	27	33	33	31
3	30	41	40	42	41
4	40	56	60	61	59
5	50	78	77	70	75
6	60	90	92	82	88
7	70	106	100	100	102
8	80	115	121	124	120
9	90	135	137	130	134
10	100	152	156	139	149
Final crack length, mm		114	102	108	108
Specimen "B" - 148 mm ligament length					
1	10	11	15	13	13
2	20	25	29	27	27
3	30	40	39	44	42
4	40	56	59	62	59
5	50	72	73	69	71
6	60	88	84	84	85
7	70	99	102	93	98
8	80	112	109	113	111
9	90	128	125	124	126
10	100	137	144	142	141
11	110	150	157	149	152
12	120	165	172	167	168
13	130	183	181	176	180
14	140	198	203	190	197
Final crack length, mm		148	142	147	146

equations can be written in the following form:

$$y = 0.460x - 1.617 \quad \text{specimen "A"} \quad (2)$$

$$y = 0.466x - 0.167 \quad \text{specimen "B"} \quad (3)$$

The coefficients m and b in Eq. 2 and 3 present average values of 3 test series. The coefficient m value multiplied by 1000 (because crack extension is given in mm and time is given in μs) represents an average, approximate crack velocity value, expressed in m/s. Coefficient b can be neglected for all impact energies, except the minimum value of E=883 J. This can be explained by variation of crack velocity in time: starting from zero value, crack velocity reaches its maximum and it decreases again to the zero value when the fracture process is

over, Bilek (6). For low impact energy the increasing crack velocity time period represents significant part of the total time, spent in fracture processes. In this way, crack velocities can be expressed as:

$$v = 460 \text{ m/s for specimens "A" and}$$

$$v = 466 \text{ m/s for specimens "B"}.$$

The difference of 6 m/s in two crack velocities can be neglected. The mean crack velocity value of 463 m/s can be accepted as the common value in these experiments.

For better description of the crack behaviour on low and high energy levels in the impact fracture processes, additional experiments are needed as it can be concluded from diagrams in Fig. 7 and 8. In the case of small extended cracks corresponding to low impact energies, a lower average crack velocity can be expected. In the case of large extended cracks, corresponding to high impact energies, crack velocity can be retarded in the final stage of fracturing, and this can be contributed to the variation in the stress state and crack resistance with the ligament length.

The temperature effect on the crack velocity is presented in Fig. 9. The plotted regression lines are obtained by calculation of m and b coefficients, using crack length and time recorded values from Tables 3 and 4. For -50°C test temperature two regression line equations, corresponding to the "A" and "B" specimens, are obtained, respectively:

$$y = 0.664x + 1.077 \quad \text{specimen "A"} \quad (4)$$

$$y = 0.717x - 0.244 \quad \text{specimen "B"} \quad (5)$$

It is clear from the Fig. 9 that the higher crack velocity and the larger crack extension are connected with the shorter initial ligament length (the case of specimen "B"). In this case, for 146 mm average final crack extension the spent time overpassed 197 μs and the calculated mean crack velocity was as high as 717 m/s, for the impact energy of 3090 J. For the same impact energy in the case of "A" specimen final crack extension of 108 mm (in average) needed more than 149 μs, and corresponding crack velocity was 664 m/s. Again, the differences in the stress state and crack resistance caused by different initial ligament lengths could be responsible for different crack velocities and final crack extensions. It is to be noted that the scatter bands for average values, marked on the diagrams, as well as for individual specimen values are reasonably narrow.

Situation is a little bit complicated in regression lines analysis when tests at room temperature are considered. For the first 70 mm in crack extension on both "A" and "B" specimens linear dependence between crack extension and time can be expressed by equations

$$y = 0.481x + 0.132 \quad \text{specimen "A"} \quad (6)$$

$$y = 0.508x + 0.382 \quad \text{specimen "B"} \quad (7)$$

and again, as in the previous case, the higher velocity of 508 m/s corresponds to the shorter ligament specimen. The scattering of linearity in that part is negligible for average, as well as for individual values. Crack velocity retardation starts to occur when crack extension overpasses 70 mm in these tests. Taking into the account all plotted points, that correspond to the crack extensions up to 80 mm in specimen "B" and up to 110 mm in specimen "A", following equations

$$y = 0.439x + 5.022 \quad \text{specimen "A"} \quad (8)$$

$$y = 0.465x + 1.148 \quad \text{specimen "B"} \quad (9)$$

can be derived. Average crack velocities for crack extensions close to the final crack extensions are noticeably lower compared to the velocities in the first 70 mm crack extension (about 439 m/s compared to 508 m/s for the shorter "A" specimen ligament and about 465 m/s compared to 481 m/s for the longer "B" specimen ligament). As already mentioned, in the case of room temperature tests with different impact energies (see Fig. 7), one can expect the crack velocity variation with the crack extension in fast fracture, when crack arrest behaviour is clearly expressed.

CONCLUSIONS

Developed crack velocity measuring device, consisted of connecting-strip foils and timer with memories, enabled the crack velocity determination in the drop weight tests, using the side-grooved fatigue precracked DCB specimens made of NIONICRAL 70 800 MPa strength class steel. Crack velocities at room temperatures vary with the crack position in fracture process. For different impact energies and different ligament lengths, crack velocities ranged between 439 m/s and 508 m/s. Tested at -50°C the same specimens exhibited crack velocities of 664 m/s and 717 m/s. Effect of initial ligament ratio on crack velocity was also observed. Additional experiments are needed for the crack behaviour explanation in the starting and closing parts of fracture process.

REFERENCES

1. Harn, G.T., Hoagland, R.G. and Rosenfield, A.R., "Fast fracture toughness of steel" in Dynamic Fracture Toughness (The Welding Institute, Cambridge, 1977)
2. Irwin, G.R., "Comments on dynamic fracture testing" in Dynamic Fracture Toughness (The Welding Institute, Cambridge, 1977)
3. Erdogan, F. "Crack propagation theories" in "Fracture", Volume II, ed. Liebowitz, H., (Academic Press, New York, 1968).
4. Hoagland, R.G., Rosenfield, A.R., Gehlen, P.C., Harn, G.T., "A crack arrest measurement procedure for K_{Ic} , K_{ID} , K_{Ia} properties, in Fast Fracture and Crack Arrest, (ASTM, STP 627, Philadelphia, 1977).
5. Knott, J.F., "Fundamentals of Fracture Mechanics", (Butterworths, London, 1973).
6. Bilek, Z., "Dynamic fracture toughness of a structural steel" in Advances in Fracture Research, Volume 2, (ECF5, Pergamon Press, Oxford, 1981).

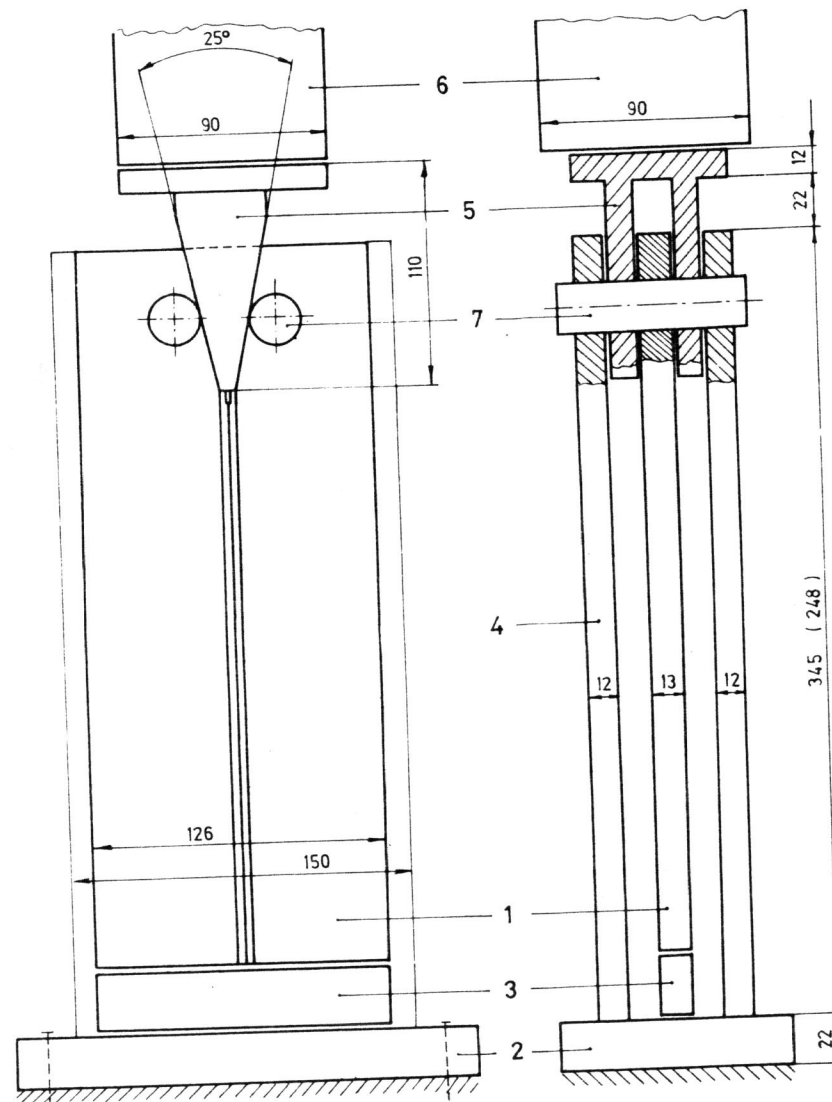


Fig. 1 Schematic presentation of drop weight impact testing system with DCB specimen

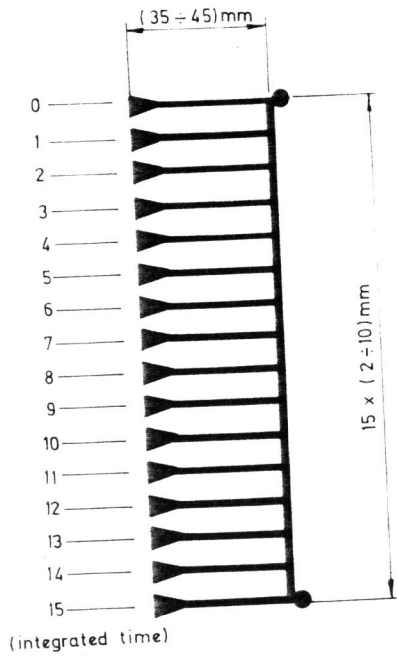
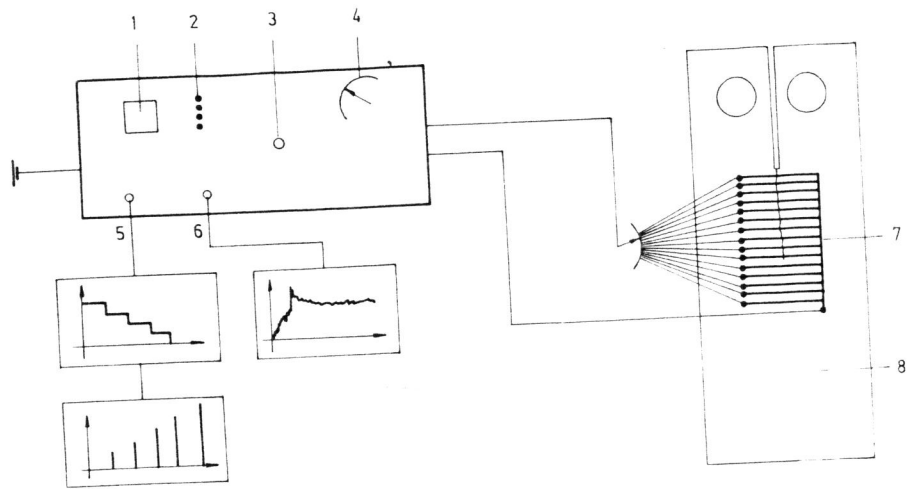


Fig. 2a Schematic view of crack velocity measuring device
b Equidistant strip marks

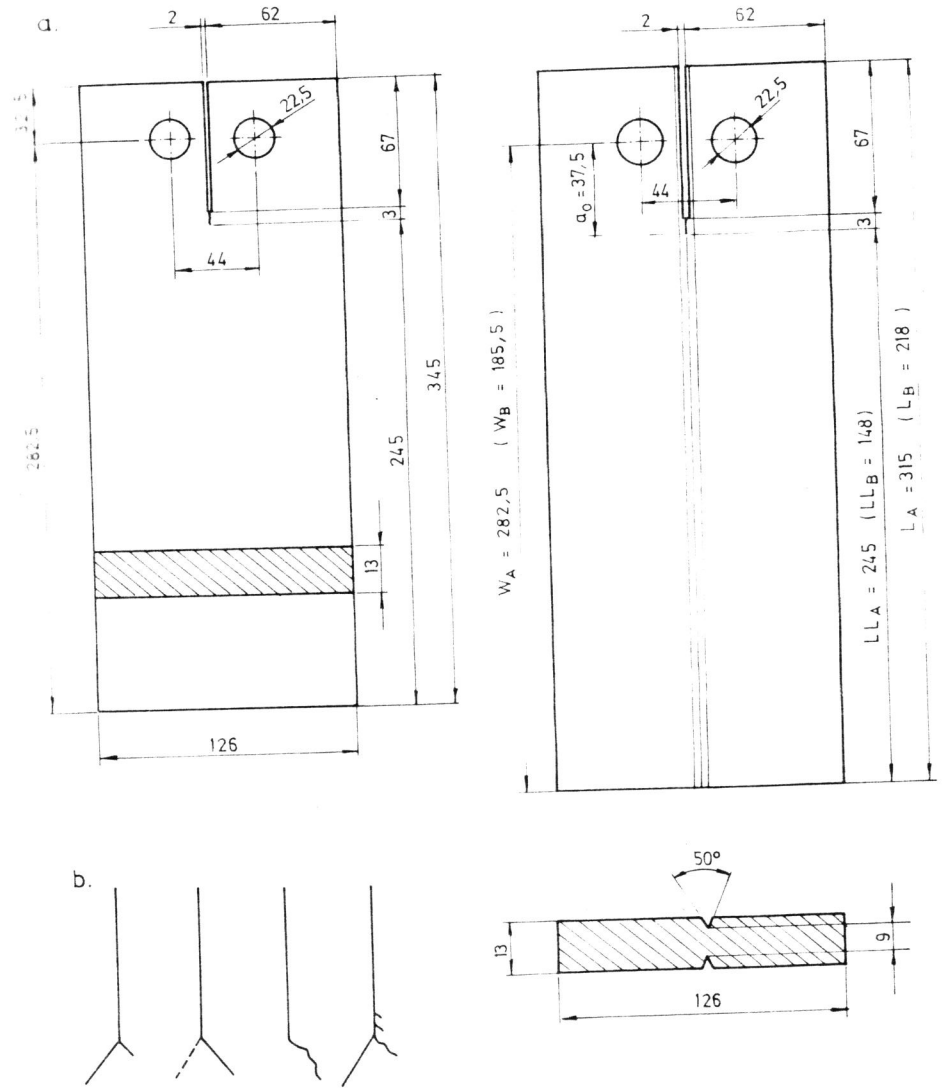


Fig. 3a DCB fatigue precracked specimen with smooth outer surfaces
b Direction of crack extension

Fig. 4 Side-grooved fatigue precracked DCB specimen of different lengths

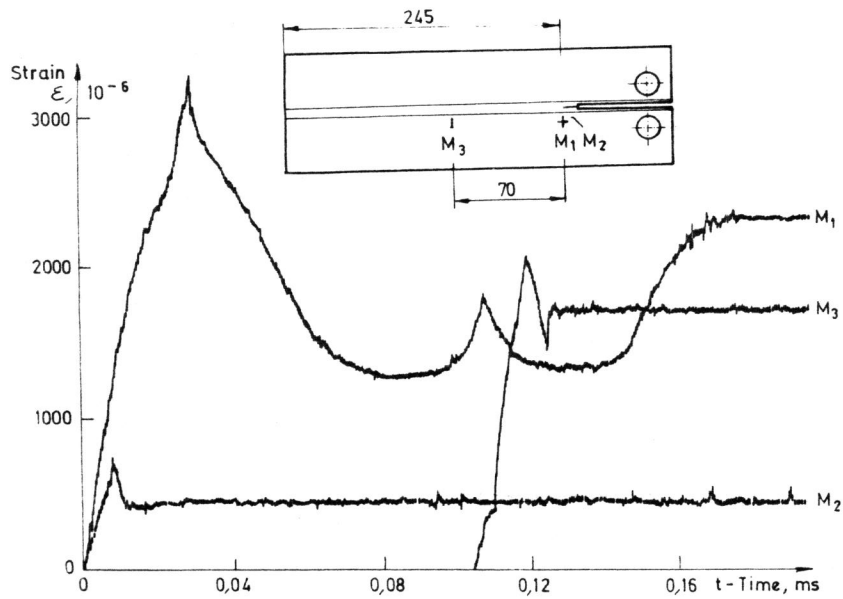


Fig. 5 Strain vs. time records for 245 mm ligament length

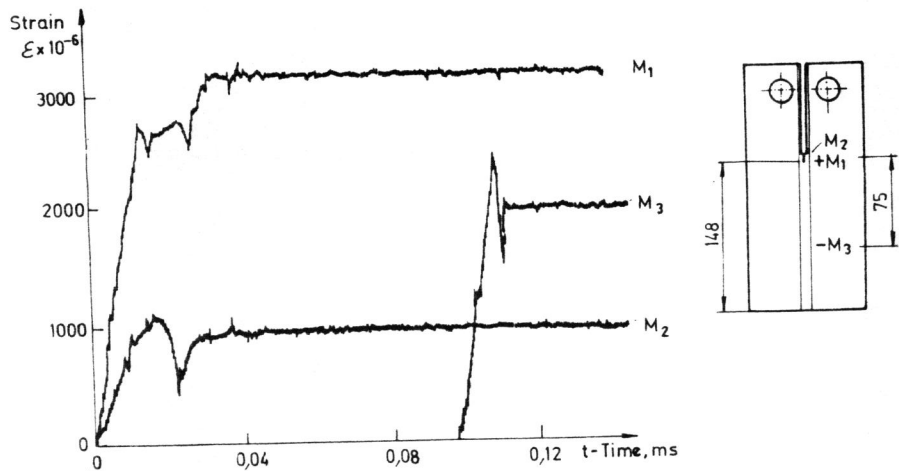


Fig. 6 Strain vs. time records for 148 mm ligament lengths

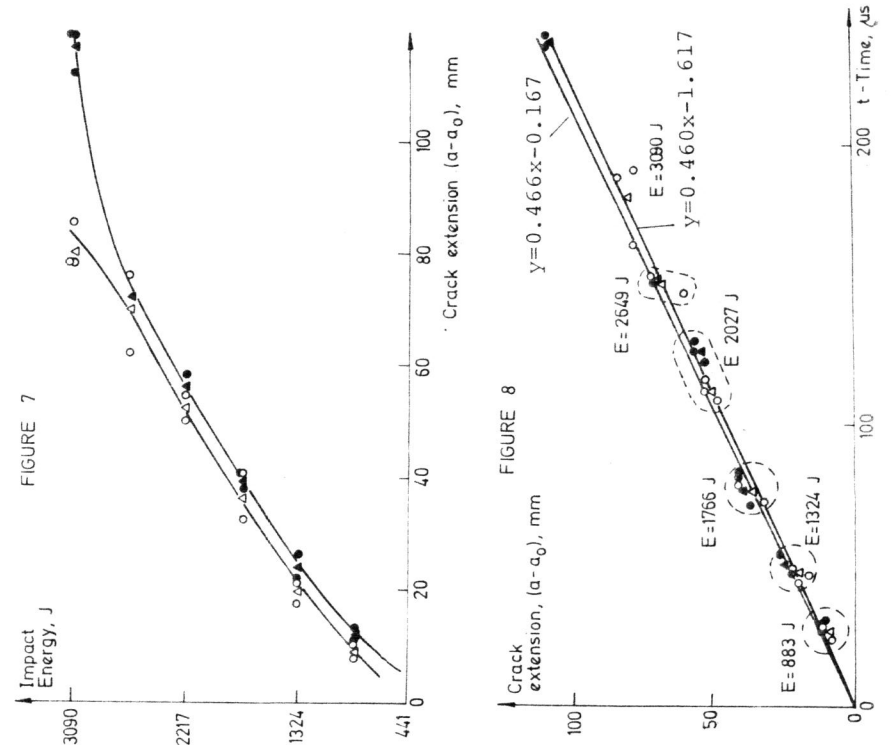


FIGURE 9

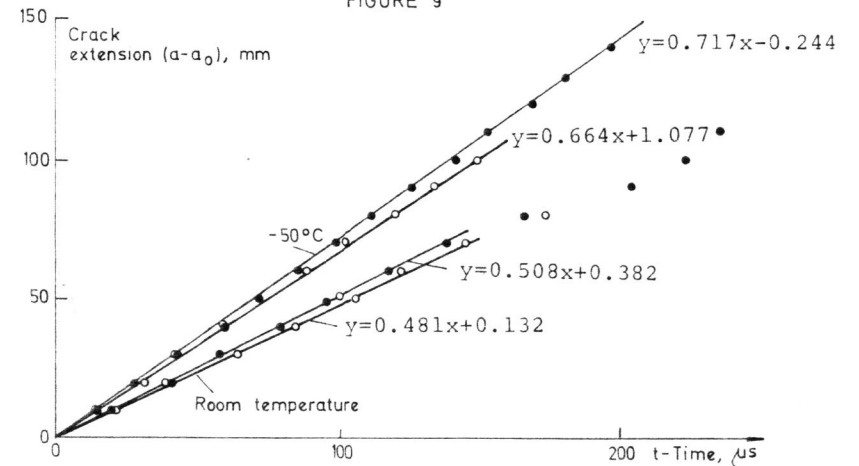


Fig. 7 Impact energy vs. crack extension for different ligament lengths specimen

Fig. 8 Crack extension vs. time for different impact energies

Fig. 9 Crack extension vs. time for different test temperatures